Surfaces and Interfaces 25 (2021) 101284

Contents lists available at ScienceDirect

Surfaces and Interfaces

journal homepage: www.sciencedirect.com/journal/surfaces-and-interfaces

Surface modification of 2-D $Ti_3C_2T_x$ for the effective capture and elimination of acetaldehyde as a co-catalyst: A theoretical and experimental study

Xiao Wang [1], Asad Mahmood [1], Gansheng Shi, Yan Wang, Guanhong Lu, Xiaofeng Xie, Jing Sun [*]

State Key Laboratory of High Performance Ceramics and Superfine Microstructure, Shanghai Institute of Ceramics, Chinese Academy of Sciences

ARTICLE INFO

Keywords:
$Ti_3C_2T_x$
Adsorption
Acetaldehyde
Surface modification
T-vacancies

ABSTRACT

As a newly explored 2-D material with metallic conductivity, Ti_3C_2 has drawn much attention as co-catalysts for the photocatalytic oxidation (PCO) of indoor air pollutants. Herein, we implement the periodic density functional theory calculations to study the interaction between Ti_3C_2 and acetaldehyde molecules and Ti atoms in Ti_3C_2 are identified as the active sites for the capture of acetaldehyde molecules. When fully saturated with surface terminators ($Ti_3C_2T_2$, T stands for -F, -O and -OH groups), the $Ti_3C_2F_2$ and $Ti_3C_2O_2$ have weak affinity to acetaldehyde while $Ti_3C_2(OH)_2$ could provide moderate adsorption strength by forming H-bonds with acetaldehyde. Creating T vacancies in $Ti_3C_2T_2$ monolayers through surface modification could effectively improve its affinity to acetaldehyde with the adsorption energy increasing from 0.281, 0.235 and 0.878 to 1.750, 1.830 and 1.960 eV for $Ti_3C_2F_x$, $Ti_3C_2O_x$ and $Ti_3C_2(OH)_x$, respectively. The positive effect of $Ti_3C_2T_x$ as a co-catalyst is also verified by constructing $Ti_3C_2T_x$-TiO_2 composite photocatalysts. The introduction of $Ti_3C_2T_x$ flakes effectively promote the PCO of acetaldehyde by improving the adsorption of target molecules and accelerate the separation of electron-hole pairs in TiO_2. This work provides a promising 2-D $Ti_3C_2T_x$ material as a co-catalyst for the capture and photocatalytic elimination of indoor air pollutants.

1. Introduction

The elimination of indoor acetaldehyde has become an important issue nowadays. As an irritant to the skin, eye, the respiratory and nervous system, acetaldehyde might be emitted by furniture, wall paint and other indoor decorations [1,2], Photocatalytic oxidation (PCO) has been proven to be an effective way in the elimination of indoor air pollutants [3-6]. Due to the low cost, high mineralization ability and broad-spectrum activity, semiconductors such as TiO_2 is commonly used in several water purification technologies [7-9]. However, unlike the organic pollutants in water, gaseous pollutants such as acetaldehyde show a much lower concentration in the indoor atmosphere [10]. The effective capture of gaseous organic molecules by photocatalysts is crucial for the subsequent PCO reaction. However, the application of many oxides-based semiconductor materials in the air purification field is limited by their intrinsic low specific surface area, which can only provide few active sites for the adsorption of gas molecules [11,12]. Besides, as a traditional direct-gap semiconductor, TiO_2 has also been criticized for the rapid recombination of photon-induced electron-hole pairs, which is detrimental for the effective utilization of sunlight and the generation of active oxidative species such as $\bullet O_2^-$ and •OH radicals [3,5,13,14].

Since the development of graphene, the family of 2-D materials has started to draw the attention of researchers in the field of photocatalysts due to their exceptional optical and electrical properties as a consequence of the reduced dimensionality [15-17]. In contrast to their bulk counter parts, 2-D materials exhibit high specific surface areas, which made them ideal catalysts or co-catalysts for the PCO of organic gaseous molecules. In recent years, MXene materials, including transition metal carbides and transition metal nitrides, have been developed as a new kind of 2-D material. Most of the MXene materials today are synthesized from MAX phases, in which M stands for early transition metals, A is a group 13 or 14 elements and X represents either C or N [18-20]. Through etching the A layer in MAX phases with HF or other etchant, single or

* Corresponding author.
E-mail address: jingsun@mail.sic.ac.cn (J. Sun).
[1] These authors contribute equally to this article.

https://doi.org/10.1016/j.surfin.2021.101284
Received 15 April 2021; Received in revised form 9 June 2021; Accepted 13 June 2021
Available online 18 June 2021

few-layered MXene could be synthesized [20,21]. As reported previously, most of the MXene materials possess a high specific surface area and metallic conductivity, which makes them promising materials for the fabrication of hybrid photocatalysts. Among the large MXene family, $Ti_3C_2T_x$ (T stands for the surface terminators), which was firstly synthesized by Yury's group in 2011 [22], has drawn lots of attention in the field of gas phase catalytic reactions [23-25]. On one hand, the large specific surface area would provide extensive active sites for the adsorption of gas molecules, on the other hand, the metallic conductivity of $Ti_3C_2T_x$ is beneficial for the effective separation of photon-induced charge carriers [26]. Li et al found that due to the existence of unsaturated Ti atoms, the surface of Ti_3C_2 could spontaneously capture CO_2 molecules through chemisorption with an E_{ads} of 0.59 eV, which was essential for the further photocatalytic reactions [26]. Due to its preference in absorbing particular target gas molecules, $Ti_3C_2T_x$ could also be applied in the separation of various gases including CO_2, He, H_2, O_2, N_2 and CH_4 [27]. $Ti_3C_2T_x$ has also been applied as a kind of co-catalyst. Yu et al built $Ti_3C_2T_x$ /TiO_2 heterojunctions for the photocatalytic reduction of CO_2 [28]. Compared with the commercial TiO_2, a 3.7-fold increase in the CH_4-production rate was observed when applying the composite as the photocatalyst. $Ti_3C_2T_x$ could not only work as a substrate for the uniform distribution of active sites, but also trap photon-induced holes from TiO_2 and inhibit the recombination of electron-hole pairs [29-31]. In addition to photocatalytic CO_2 reduction, $Ti_3C_2T_x$ /TiO_2 hybrid photocatalysts have also been applied in water splitting [32-34] and water purification [35-37]. In both cases, $Ti_3C_2T_x$ would effectively enhance the charge separation in TiO_2 due to its metallic conductivity. As a great candidate for constructing heterojunctions with TiO_2, $Ti_3C_2T_x$ may have great potential in the PCO of gas pollutants such as indoor acetaldehyde.

However, due to the existence of unsaturated Ti atoms, the surface of pure Ti_3C_2 is not stable in most cases. According to the type of etchants applied in the exfoliation process, various surface functional groups such as -F, -O and -OH groups would attach to the surface of Ti_3C_2 to form $Ti_3C_2T_2$ (T represents F, O, and OH groups). The existence of these surface termination groups may cause a distortion in the lattice structure of Ti_3C_2 and influence its conductivity, as well as the adsorption behavior of guest molecules[38-40]. As Ti_3C_2 could act as the acceptor of photon-induced charge carriers and the provider of active sites for the capture of gaseous acetaldehyde molecules, the existence of surface terminations might have a great impact on the performance of hybrid photocatalysts based on Ti_3C_2. Unlike other 2D materials, the amount and distribution of functional groups on the surface of Ti_3C_2 could be easily tuned by hydrothermal treatment, thermal annealing, plasma treatment and adjusting the etching or exfoliation environment. In 2011, Gogotsi et al. found that when etching Ti_3AlC_2 with HF in an aqueous solution, -OH and -F were the dominant surface terminator [41]. The results reported by Alshareef et al. revealed that extending the etching time would induce an increase in the amount of both -OH and -F terminators [42]. By replacing water with polar organic solvents during the etching process, Barsoum et al. synthesized $Ti_3C_2T_x$ flakes rich in -F terminators [43]. Xu et al. hydrothermally treated $Ti_3C_2T_x$ with alkali solution and revealed that -F and -OH terminal groups were replaced by -O groups during the high-temperature alkalization process [44]. Besides, researchers also found that hydrogen plasma [45] and thermal treatment under inert gas [46] or vacuum [47] would cause a partial removal of O groups and the exposure of Ti atoms. STEM images reported by Persson et al. revealed that the desorption of surface termination groups at high temperatures would result in uncovered sites on the surface of $Ti_3C_2T_x$ [47]. The modification of surface functional groups would impact the electronic properties of $Ti_3C_2T_x$ and its ability in capturing target gas molecules, which opens a possibility for the optimization of hybrid photocatalysts constructed on the basis of $Ti_3C_2T_x$. Besides, as reported by Tang et al., by removing part of surface terminators in $Ti_3C_2T_x$, a higher hydrophobicity can be achieved, which improves the stability of $Ti_3C_2T_x$ flakes in air [46] and favors its application in gas sensors and photocatalysis. However, the impacts of surface modification are still not thoroughly understood. Besides, most of the computational works today mainly concentrate on the adsorption and photocatalytic reaction of inorganic molecules such as CO_2, N_2, NH_3 et al. [27]. The adsorption behavior of typical VOCs such as acetaldehyde on the surface of $Ti_3C_2T_x$ and the interaction mechanism were still unclear.

Herein, the adsorption behavior of acetaldehyde molecules on various $Ti_3C_2T_x$ was explored through first-principal simulation. By comparing the adsorption energy of different configurations, the adsorption model of acetaldehyde molecules on the surfaces were determined. The electrical properties and the band structure of Ti_3C_2 with and without surface termination groups were simulated to verify the influence of the terminators on the electron transportation and the adsorption behavior of target molecules. T-vacancies are constructed by removing the surface groups and their influence the adsorption behavior of acetaldehyde molecules is studied. Photocatalytic experiments are carried out by constructing $Ti_3C_2T_x$-TiO_2 composite for the PCO of acetaldehyde. This work would provide theoretical and experimental evidences for the application of $Ti_3C_2T_x$ as a co-catalyst for the PCO of indoor acetaldehyde.

2. Computational details

First principal calculations in this work were performed via Vienna *ab-initio* Simulation Package (VASP) and a projected augmented wave method was applied to treat the valence and core electrons [48]. We started from the crystal structure of Ti_3AlC_2 bulk crystal. Initially, the crystal structure of Ti_3AlC_2 was fully relaxed in a $2 \times 2 \times 1$ supercell generalized-gradient-approximation (GGA) given by Perdew-Burker-Erzhenhof (PBE) as exchange correlation functions with a cutoff energy of 400 eV [49,50]. Next, the Al atoms were removed from the bulk lattice and optimized again under similar optimization parameters. Next, the surface was cleaved along the [001] direction and expanded in $3 \times 3 \times 1$ supercell to produce the monolayer surface model. The Ti_3C_2 monolayer was first optimized with different cutoff energy values, i.e., 300, 400, 500, 600, 700 eV, where the 400 eV value produced maximum stability and low enthalpy of formation. Also, not much difference could be observed in the density of states (not given), thus we selected 400 eV as the optimum cutoff energy value, which gives reliable results at low computational cost. The geometry optimization of the slab models was carried out using GGA-PBE level theory to account for the weak van der Waals forces, the Grimme function (DFT-D3) was used. The k-points were sampled in the MonKhorst pack grid as $4 \times 4 \times 1$ for geometry optimization [51]. The k-point mesh sample was kept as $12 \times 12 \times 1$ for band structure and the density of states calculation, which were optimized before applying to all models. A vacuum of 20 Å was used for the geometry optimization and properties calculations. The clean Ti_3C_2 monolayer was decorated on both sides by same number of desired functional groups, i.e., O, OH, and F. We also tested the vacancy behavior in functional groups. The dipole correction method was also tested for the defective surface model; however, it did not affect the final results thus we used non-dipole corrected models. All the atoms were allowed to relax during calculations and no atomic constraints were applied otherwise mentioned. The convergence criteria were as follows: energy $= 5.0 \times 10^{-6}$ eV/atom, maximum force $= 0.01$/Å, maximum displacement $= 5.0 \times 10^{-4}$ Å. An ultra-soft pseudopotential was used for the structural relaxation and properties calculations. The following electronic configuration was used for different elements; Ti: [Ne] 3s [2] 3p [6], C: [He] 2s [2] 2p [6], O: [He] 2s [2] 2p [6], F: [He] 2s [2] 2p [6], H: 1s [1]. The clean surface model contained 45 number of atoms. The functional groups containing model contained 63, 63, and 82 number of atoms corresponding to O, F, and OH functional groups. The acetaldehyde molecule was also optimized in the gas phase in a box exhibiting similar dimensions. Different configurations of the acetaldehyde molecule were used to identify the site selective interaction, while the most

stable configurations were further used for the calculation of DOS and electron density difference (EDD). The adsorption energy was calculated as follows:

$$E_{ads} = E_{molecule/surface} - E_{molecule} - E_{surface} \quad (1)$$

where, $E_{molecule/surface}$ is the energy of the adsorption complex, $E_{molecule}$ is the energy of the acetaldehyde in the gas phase, and $E_{surface}$ is the energy of the clean surface.

3. Results and discussion

3.1. Geometric structures of Ti_3C_2 and acetaldehyde

The structure of Ti_3C_2 with a clean surface is optimized through GGA-PBE as the exchange correlation function (Fig. S1). Two kinds of Ti atoms exist in the pristine Ti_3C_2 crystal lattice: the octahedral coordinated ones constituting the inner layer (noted as Ti_{6c}) and the unsaturated ones on the surface layer (with a coordination number of 3), which are designated as Ti_{3c}. The surface of pure Ti_3C_2 is composed of 3-fold under-coordinated Ti atoms and 6-fold carbon atoms (noted as C_{6c}). The average bond length of Ti_{3c}-C_{6c} on the surface is 2.049 Å, which is 6.9% shorter than the bond length of Ti_{6c}-C_{6c} (2.202 Å), suggesting a relatively stronger interaction between the unsaturated Ti_{3c} and C_{6c} atoms. The acetaldehyde molecule is also relaxed in a similar supercell to achieve a geometrically stable configuration (Fig. S2). After geometry optimization, the lengths of the C-C and C=O bonds in an acetaldehyde molecule are 1.502 Å and 1.226 Å, respectively.

Ti_3C_2 has been regarded as an ideal co-catalyst for it could accept the photon-generated electrons from photocatalysts due to it good conductivity. As illustrated by the density of states (DOS) of Ti_3C_2 with a clean surface (Fig. S1b), the valance and conduction band of Ti_3C_2 overlapped at the Fermi level, showing the metallic properties of Ti_3C_2. Ti atoms are supposed to have the dominant contribution to the states around the Fermi level. Fig. S1c and S1d further indicate that the 2p-states of C_{6c} atoms mainly contributed to the conduction band (CB) while the valence band (VB) is mainly composed of the 3d-states of Ti atoms.

3.2. Adsorption behavior of acetaldehyde molecules on Ti_3C_2

In order to simulate the adsorption behavior of acetaldehyde on the surface of Ti_3C_2, acetaldehyde molecules with different orientations are considered (Fig. S3). In all of the cases, acetaldehyde molecules are captured by the strong interaction between the carbonyl O in acetaldehyde and unsaturated surface Ti_{3c} atoms of Ti_3C_2. The adsorption energy is calculated for all the configurations to figure out the most stable adsorption mode. TCA_IV shows the highest E_{ads} of 3.60 eV, followed by TCA_II (3.52 eV), TCA_V (3.34 eV), TCA_I (3.28 eV) and TCA_III (2.17 eV) (Table 1). As reported by Guo et al., the solid surface could effectively capture gas molecules when the adsorption energy exceeded 0.5 eV [52]. The high E_{ads} between acetaldehyde molecules and Ti_3C_2 makes it a great candidate for capturing target molecules in the photo-elimination of acetaldehyde. In TCA_IV, the carbonyl O would bond with three adjacent Ti atoms with bond lengths of 2.070 Å, 2.055 Å and 2.772 Å (Table 2). The strong interaction between the molecule and the surface induces the re-distribution of electrons, which leads to obvious deformation in both the acetaldehyde molecule and the lattice structure of Ti_3C_2. Compared with free acetaldehyde molecules in the gas phase, the bond length of C=O increases (19.4%) from 1.226 Å to 1.464 Å while the bond length of surface Ti-C increases (2.24%) from 2.050 Å to 2.095 Å. Similar as TCA_IV, O atoms could also interact with three Ti atoms in the configuration of TCA_II, TCA_III and TCA_V by forming Ti-O bonds. On the contrary, only one Ti-O bond forms in the configuration TCA_I, but with a relative smaller bond length of 1.872 Å. The interaction between carbonyl O in acetaldehyde and unsaturated Ti atoms on the surface of Ti_3C_2 plays an important role in the adsorption process and the unsaturated Ti atoms provide large number of active sites for the adsorption of acetaldehyde molecule, which might also be beneficial for the effective capture gaseous molecules. However, the relative strong interaction between the target molecule and the photocatalyst may also hinder the desorption of mid-product during the PCO process and lead to the de-activation of the photocatalyst.

Table 1
adsorption energy of various adsorption configurations of acetaldehyde on the surface of Ti_3C_2, $Ti_3C_2T_2$ and $Ti_3C_2T_x$.

	Conf_I	Conf_II	Conf_III	Conf_IV	Conf_V	Conf_VI
Ti_3C_2	3.28 eV	3.52 eV	2.17 eV	3.60 eV	3.34 eV	\
$Ti_3C_2F_2$	0.28 eV	0.25 eV	0.23 eV	0.23 eV	0.21 eV	0.17 eV
$Ti_3C_2O_2$	0.21 eV	0.17 eV	0.19 eV	0.11 eV	0.22 eV	0.24 eV
$Ti_3C_2(OH)_2$	0.83 eV	0.64 eV	0.79 eV	0.24 eV	0.88 eV	
$Ti_3C_2F_x$	1.70 eV	1.75 eV	0.22 eV	1.59 eV		
$Ti_3C_2O_x$	1.78 eV	1.83 eV	0.27 eV	1.66 eV	0.19 eV	1.61 eV
$Ti_3C_2(OH)_x$	0.61 eV	1.96 eV	0.69 eV	0.37 eV	0.72 eV	

The chemisorption of acetaldehyde molecules also causes a re-distribution of electrons between the surface and the gas molecule. According to the EDD results of TCA_V in Fig. 1b, charge transfer mainly happens between the carbonyl O atoms in acetaldehyde and the surface Ti atoms. O atoms would attract electrons from adjacent Ti atoms and induce electron depletion areas around them. The re-distribution of electrons caused by the adsorption of acetaldehyde might weaken the surface Ti_{3c}-C_{6c} bonds but strengthen the Ti_{6c}-C_{6c} bonds in the inner layer of Ti_3C_2. In addition to the lattice structure, the re-distribution of electrons would also influence the band structure of Ti_3C_2. As illustrated by Fig. 1c and Fig. S4, the adsorption of acetaldehyde would induce distinct states in the energy range around 2.5 eV by causing a difference in the 3d-states of Ti atoms. However, no obvious change in the DOS around the Fermi level of Ti_3C_2 is observed. Therefore, the adsorption of acetaldehyde molecules does not have a noticeable impact on the metallic conductivity of Ti_3C_2. Photon-induced charge carriers generated in the semiconductors could still migrate into Ti_3C_2 and react with the absorbed O_2 or H_2O molecules to form active radicals. Besides, due to the strong interaction between acetaldehyde molecules and the surface Ti atoms, photon-induces holes that migrate into Ti_3C_2[29-30] might directly oxidize the adsorbed acetaldehyde molecules. Based on the above results, Ti_3C_2 could be regarded as an ideal candidate for constructing hybrid photocatalysts with other semiconductors for the PCO of gas phase acetaldehyde, but the quite strong interaction between acetaldehyde and Ti_3C_2 may limit its application due to difficulties in the desorption of mid-products.

3.3. Geometry and electronic structure of $Ti_3C_2T_2$ surfaces

Despite all the advantages, the application of Ti_3C_2 is still limited by its poor stability in air due to the large amount of unsaturated metal sites on the surface. Instead of pure Ti_3C_2 with a clean surface, most of the

Table 2
The bond lengths between carbonyl O and surface Ti or H atoms.

		Ti-Carbonyl O	H-Carbonyl O
Ti_3C_2	Ti-I	2.070	/
	Ti-II	2.055	/
	Ti-III	2.772	/
$Ti_3C_2(OH)_2$	H-I	/	1.638
	H-II	/	1.890
$Ti_3C_2F_x$	Ti-I	2.168	/
	Ti-II	2.156	/
	Ti-III	2.285	/
$Ti_3C_2O_x$	Ti-I	2.471	/
	Ti-II	2.271	/
	Ti-III	2.329	/
$Ti_3C_2(OH)_x$	H-I	2.155	1.020
	H-II	2.082	1.605

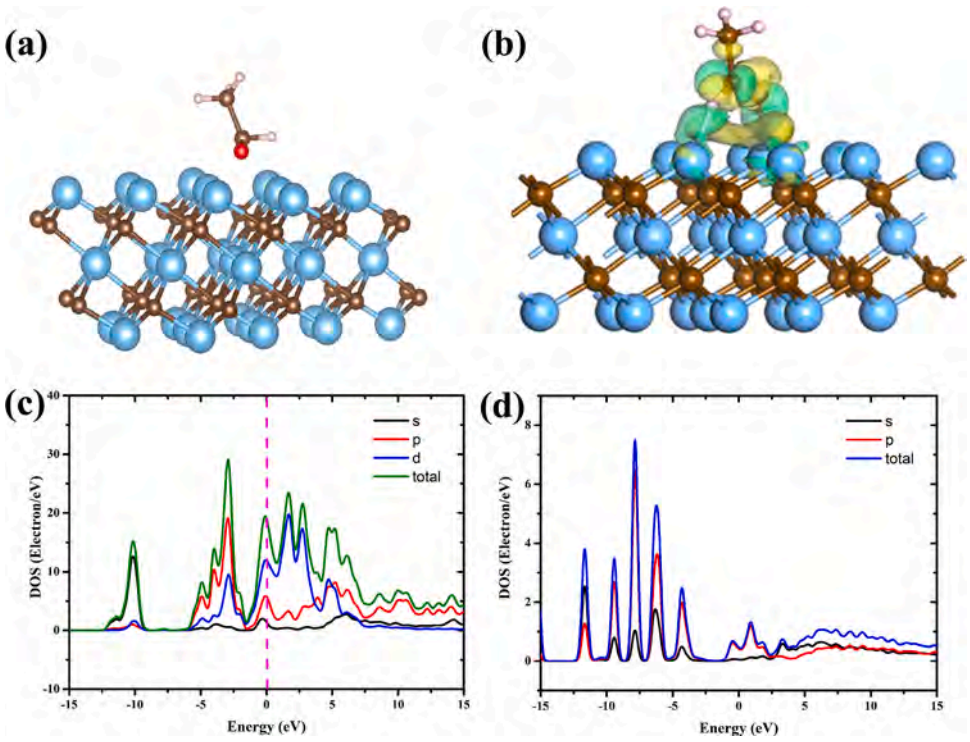

Fig. 1. (a) the side view and (b) charge density difference for the TCA_IV complex; The DOS of the surface of Ti_3C_2 and acetaldehyde molecule in the TCA_IV complex.

Ti_3C_2 synthesized through etching Ti_3AlC_2 are terminated with -F, -O or -OH groups, depending on the synthesis environment [38,47]. The existence of these termination groups would not only cause a change in the band structure of Ti_3C_2 by influencing the distribution of electrons, but also influence the adsorption behavior of acetaldehyde molecules by covering active Ti sites. Fully relaxed Ti_3C_2 surfaces terminated with different functional groups and associated density of states (DOS) are given in Fig. 2. As reported previously, there are different modes when considering the organization of surface terminators: all placed at the hollow sites vertically above the Ti_{6c} atoms (Configuration_a), all placed at hollow sites above the C atoms in the inner layer of Ti_3C_2 (Configuration_b) and the combination of the above two circumstances (Configuration_c). Among the three configurations, Configuration_a is proven to be the most thermodynamically stable one [38,39]. Therefore, the top and bottom terminators are placed at these sites for all the cases. eVen though F atoms have higher electronegativity, the bond between -O terminators and surface Ti atoms are much stronger with smaller bond lengths, which is in line with the results reported previously [53]. The bond length between surface Ti and F atoms is calculated to be 2.16 Å while the length of Ti-O bonds in $Ti_3C_2O_2$ and $Ti_3C_2(OH)_2$ are 1.98 Å and 2.18 Å, respectively.

Compared with pure Ti_3C_2, both changes in the lattice configuration and the density of states are observed in $Ti_3C_2T_2$. For $Ti_3C_2F_2$, the bond length between surface Ti and F atoms is calculated to be 2.16 Å and the average bond length of Ti_{3c}-C_{6c} in the surface layer increases (1.37%) from 2.048 Å to 2.076 Å while the average bond length of Ti_{6c}-C_{6c} decreases (1.08%) from 2.204 Å to 2.180 Å. As a termination group, the F element is expected to obtain electrons from the adjacent Ti atoms, which weakens the Ti_{3c}-C_{6c} bonds but strengthens the Ti_{6c}-C_{6c} bonds at the same time [39]. Similarly, -O and -OH terminators would also bond

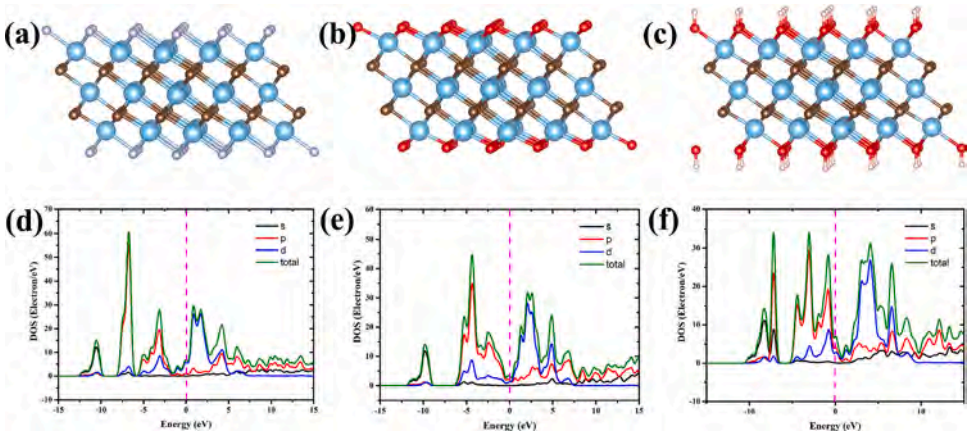

Fig. 2. Optimized structure of the side view of (a) $Ti_3C_2F_2$, (b) $Ti_3C_2O_2$ and (c) $Ti_3C_2(OH)_2$. The Ti and C atoms in $Ti_3C_2T_2$ were in the color of blue and brown, respectively. F atoms in $Ti_3C_2F_2$ were colored in light blue. H atoms in $Ti_3C_2(OH)_2$ were colored in pink. O atoms in $Ti_3C_2O_2$ and $Ti_3C_2(OH)_2$ were colored red. DOS of (d) $Ti_3C_2F_2$, (e) $Ti_3C_2O_2$ and (f) $Ti_3C_2(OH)_2$.

with Ti atoms on the surface and the bond lengths are ~1.99 Å and ~2.18 Å, respectively. The bond length of Ti_{3c}-C_{6c} in the surface layer changes from 2.048 Å to 2.210 Å and 2.080 Å while the bond length of Ti_{6c}-C_{6c} changes from 2.204 Å to 2.169 Å and 2.191 Å due to the addition of -O and -OH terminators. Compared with -OH and -F groups, -O terminators have the largest impact on the lattice structure of Ti_3C_2, which is in accordance with the strong interaction between surface Ti and O atoms. In addition to the lattice structure, the addition of different termination groups would also influence the electronic structure of Ti_3C_2 by causing a re-distribution of the electrons. According to the corresponding DOS for the surface of $Ti_3C_2F_2$, $Ti_3C_2O_2$ and $Ti_3C_2OH_2$ (Fig. 2), all the surfaces are conductors and the conductivity is mainly provided by the d-orbitals of Ti atoms. Compared with the DOS of pure Ti_3C_2 in Fig. S1, new bands appears in the DOS of $Ti_3C_2F_2$ between -8 and -5 eV while the band at the Fermi level decreases. As shown by the PDOS overlap pattern of the elements in Fig. S5, the p-states of F have a large overlap with those of Ti atoms, indicating that the bond between F and surface Ti atoms is the main cause for the change in the electronic properties of Ti_3C_2. Similarly, the addition of -O and -OH terminations also decreases the DOS of Ti_3C_2 around the Fermi level. Among the three derivatives, $Ti_3C_2O_2$ shows the smallest DOS at the Fermi level, indicating that the addition of -O terminators may harm the conductivity of Ti_3C_2, which is unfavorable for the transfer of photon-induced charge carriers.

3.4. Adsorption of acetaldehyde molecules on $Ti_3C_2T_2$

The adsorption configuration and energy of acetaldehyde molecules on different surfaces are also calculated to compare the performance of different surfaces in capturing pollutant molecules. The most stable adsorption configurations are obtained by simulating different configurations of $Ti_3C_2T_2$-acetaldehyde complexes(Fig. S6, S7 and S10). Compared with pure Ti_3C_2, the adsorption of acetaldehyde molecules on the surface of $Ti_3C_2F_2$ and $Ti_3C_2O_2$ are more like physical adsorption with the adsorption energy (E_{ads}) lower than 0.3 eV (Table 1). Instead of the vertical adsorption configurations in pure Ti_3C_2, horizontal adsorption modes with C-C bonds parallel to the surface of $Ti_3C_2F_2$ and $Ti_3C_2O_2$ are found to be the most stable configurations. The highest adsorption energy is calculated to be 0.281 eV and 0.235 eV for $Ti_3C_2F_2$ and $Ti_3C_2O_2$. No obvious re-distribution of electrons nor changes in the PDOS of Ti or C atoms are observed in $Ti_3C_2F_2$ and $Ti_3C_2O_2$ after the addition of acetaldehyde molecules (Fig. S8 and S9), which is in accordance with the weak interaction with acetaldehyde. On the contrary, $Ti_3C_2(OH)_2$ shows a much stronger affinity to acetaldehyde molecules with the adsorption energy of 0.878 eV, higher than the energy needed for the capture of gas molecules. As given by Fig. 3a, the addition of acetaldehyde causes an deformation in adjacent -OH groups, indicating the formation of H-bond interaction between the H atoms in OH terminators and the carbonyl O atoms. As shown by charge density differences (EDD) results in Fig. 3b, carbonyl O would attract electrons from adjacent H atoms and form an electron-rich area (green area), while leaving an electron-depletion area (yellow area) around the H atoms in OH groups, which further confirms the formation of H-bonds between the molecules and the $Ti_3C_2(OH)_2$ surface. As a result of the re-distribution of electrons, the adsorption of acetaldehyde would also influence the DOS of the surfaces. As given in Fig. 3, the adsorption of acetaldehyde on $Ti_3C_2(OH)_2$ induces new bands at the energy level of around -5.5 eV, which is mainly attribute to the change in the PDOS of O and H on the surface (Fig. S9i) caused by the H-bond interaction between carbonyl O and $Ti_3C_2(OH)_2$.

Compared with pure Ti_3C_2, the T-saturated derivatives inherit the metallic properties of Ti_3C_2 monolayer but have a much weaker affinity to gas phase acetaldehyde due to the coverage of active surface Ti sites. Among the three native derivatives, $Ti_3C_2F_2$ and $Ti_3C_2O_2$ could only form physical interaction with acetaldehyde, makes them undesirable co-catalyst for the PCO of gas phase acetaldehyde. Interestingly, the adsorption of acetaldehyde by $Ti_3C_2(OH)_2$ presents a completely different mechanism from either pure Ti_3C_2 or the derivatives terminated by -F and -O groups. The H- bond interaction between carbonyl oxygen and H atoms in surface -OH groups enables the spontaneous capture of acetaldehyde through chemical adsorption. Compared with Ti_3C_2, the moderate adsorption energy between acetaldehyde and $Ti_3C_2(OH)_2$ might be more suitable for the PCO of acetaldehyde. The large specific surface area, metallic conductivity, moderate affinity to acetaldehyde and high stability in air make $Ti_3C_2(OH)_2$ a better co-catalyst among the T-saturated Ti_3C_2 monolayers.

3.5. The effects of T-vacancies on the intrinsic properties of $Ti_3C_2T_x$ surfaces and the adsorption of acetaldehyde

Previous experimental results revealed that the distribution of T-termination groups on the surface of Ti_3C_2 could be easily tuned though surface modification process such as plasma treatment, chemical treatment or thermal annealing, which opens up the possibility to optimize the performance of hybrid photocatalyst by surface modification. Herein, we further study the influences of T-vacancies on the intrinsic properties of $Ti_3C_2T_2$ and its affinity to acetaldehyde molecules.

Fig. S11 and S12 gives the DOS of $Ti_3C_2T_x$ derivatives and the PDOS of Ti, C and corresponding termination groups. Unlike the results reported by Romer et al., in which the conductivity could be controlled through surface treatment methods like plasma treatment, no obvious differences the overall electronic properties of $Ti_3C_2T_x$ is observed when introducing isolate T deficiencies. This inconsistency might be result from the amount and distribution of the uncovered sites. Only one isolated surface termination group is extracted from our simulation model while the surface treatment may induce continuous uncovered area on the surface of $Ti_3C_2T_x$.

The adsorption energy of different absorption configurations is compared (Fig. S13~15 and Table 1) to identify the most stable adsorption complex. Compared with the fully T-saturated $Ti_3C_2T_2$ monolayers, the introduction of appropriate T vacancies would effectively facilitate the capture of acetaldehyde molecules. The adsorption energy of acetaldehyde on the surface of $Ti_3C_2F_x$ and $Ti_3C_2O_x$ are 1.75 eV and 1.83 eV, respectively, much higher than $Ti_3C_2F_2$ and $Ti_3C_2F_2$ but lower than bare Ti_3C_2. The increased adsorption energy compared with $Ti_3C_2F_2$ and $Ti_3C_2O_2$ are attributed to the electron-rich region created by

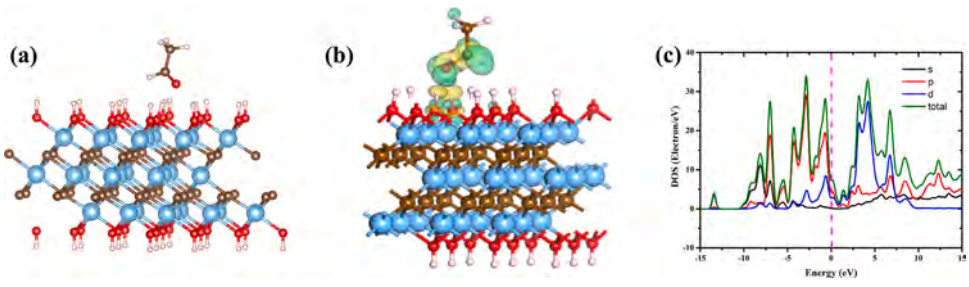

Fig. 3. (a) the most stable adsorption configuration, (b) the charge density difference and (c) the DOS of $Ti_3C_2(OH)_2$- acetaldehyde complex.

-F or -O vacancies, which would bond with the carbonyl O in acetaldehyde. Carbonyl O atoms would attract electrons from the vacancies and bond with surface Ti atoms with bond lengths of 2.285 Å, 2.156 Å and 2.168 Å for $Ti_3C_2F_x$ and 2.471 Å, 2.271 Å and 2.329 Å for $Ti_3C_2O_x$ (Table 2). In addition to bonding with surface Ti atoms, the addition of acetaldehyde would also cause a slight distortion in the position of adjacent -F groups. The lengths of Ti-F bonds around the acetaldehyde molecule are calculated as ~2.19 Å, slightly higher compared with the Ti-F bonds in pure $Ti_3C_2F_x$ (~2.15 Å). On the contrary, no such phenomenon could be observed in the case of $Ti_3C_2O_x$. DOS of the surface after the adsorption of acetaldehyde have also been calculated to further understand the adsorption mechanism. As shown by Fig. S16 and Fig. S17, the adsorption of acetaldehyde significantly influences the PDOS of Ti atoms in the energy range of -10~-2 eV for $Ti_3C_2F_x$ and -2~2 eV for $Ti_3C_2O_x$, which further confirms the formation of bonds between carbonyl O and surface Ti. EDD results also confirm the electron transfer between surface Ti and carbonyl O atoms (Fig. 4h). Carbonyl O attracts electrons from Ti and results in an electron-rich area around the carbonyl O and an electron-depletion region at the T vacancy.

The adsorption energy also increases for the $Ti_3C_2(OH)_x$-acetaldehyde complex (~1.96 eV) with the -OH vacancy working as the adsorption site. Unlike the surface of $Ti_3C_2F_x$ and $Ti_3C_2O_x$, the capture of target gas molecule is achieved through the interaction between -OH group and carbonyl oxygen. Noticeable deformation could be seen in the -OH bonds around the carbonyl O of acetaldehyde with the bond length increasing from 0.977 Å to 1.593 Å. Significant changes in the PDOS of -OH groups happens after the adsorption of acetaldehyde molecules, also confirms the formation of H-bonds between the -OH groups and the carbonyl oxygen. Almost no difference is seen in the partial density of states of surface Ti atoms, meaning there is no interaction between carbonyl oxygen and surface Ti atoms. In addition to the electron transfer between H atoms in -OH groups and carbonyl O in acetaldehyde, O atoms in -OH groups would also attract electrons from H in acetaldehyde (Fig. 4i), which induces a deformation in the molecular structure of acetaldehyde. The unique interaction between functional groups and target molecules may enable the selective adsorption and elimination of specific gas pollutants.

As indicated by the results, creating T-vacancies in $Ti_3C_2T_2$ is an effectively way in accelerating the adsorption of acetaldehyde by inducing local electron-rich areas. $Ti_3C_2F_x$ and $Ti_3C_2O_x$ would absorb acetaldehyde molecules through the charge transfer between carbonyl O and the vacancy sites while $Ti_3C_2(OH)_x$ could capture acetaldehyde by forming H-bonds. Though exhibiting different adsorption modes, the adsorption energy of acetaldehyde on the $Ti_3C_2T_x$ surfaces are similar from 1.75 eV to 1.96 eV. Unlike pure Ti_3C_2, which is not stable under in air due to the large amount of unsaturated Ti atoms, $Ti_3C_2T_x$ could provide not only stable surfaces, but also moderate adsorption energies for the capture of acetaldehyde, which make them promising candidate for constructing composite photocatalysts for the PCO of acetaldehyde.

3.6. The adsorption and PCO of acetaldehyde on $Ti_3C_2T_x$-TiO_2

In the purpose of verifying the performance of $Ti_3C_2T_x$ as a co-catalyst, $Ti_3C_2T_x$-TiO_2 composites are synthesized and applied in the photocatalytic degradation of acetaldehyde. As given by Fig. S18a and S18c, single or few layer $Ti_3C_2T_x$ is obtained by using TMAOH as the intercalation reagent. After mixing with TiO_2, thermal treatment at 300°C under Argon is carried out to remove the residue cations of the intercalant (TMA^+) and part of the surface terminators. Fig. S18b and S18d give the TEM and HRTEM images of 1.5 wt% $Ti_3C_2T_x$-TiO_2, in which the lattice structures of both TiO_2 and $Ti_3C_2T_x$ are observed, confirming the successive synthesis of $Ti_3C_2T_x$-TiO_2 photocatalyst. The impact of $Ti_3C_2T_x$ flakes on the BET specific surface area (BET-SSA) of the composite is also analyzed. As given by Table S2, due to the low weight ratio of $Ti_3C_2T_x$ flakes, only a slight increase is seen in the BET-SSA of the composites. However, when applied in the adsorption of acetaldehyde, the $Ti_3C_2T_x$-TiO_2 composites shows much better adsorption ability toward acetaldehyde and the amount of acetaldehyde absorbed on the surface of 1.5 wt% $Ti_3C_2T_x$-TiO_2 is more than twice of pure TiO_2 (Fig. 5a and Table S2). The enhanced adsorption is in accordance with the computational results above, which reveals the high affinity between surface Ti atoms and acetaldehyde molecules. In addition to the adsorption of acetaldehyde, the photocurrent density of various samples are also compared to confirm the positive effect of

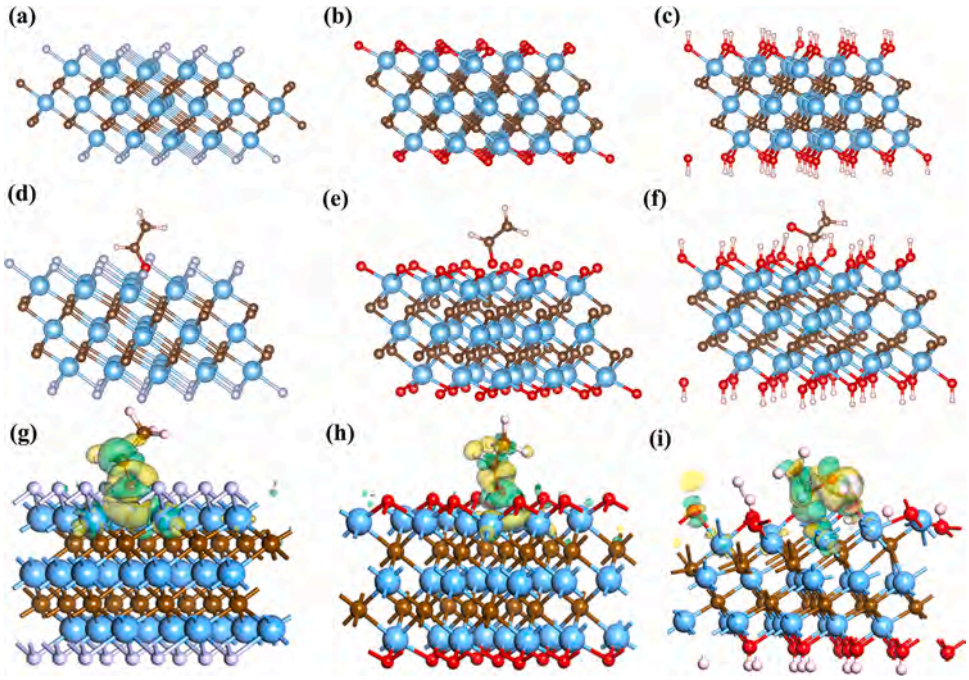

Fig. 4. Optimized structure of the side view of (a) $Ti_3C_2F_x$, (b) $Ti_3C_2O_x$ and (c) $Ti_3C_2(OH)_x$. The most stable adsorption configuration and charge density difference of acetaldehyde molecules on the surface of (d, g) $Ti_3C_2F_x$, (e, h) $Ti_3C_2O_x$ and (f, i) $Ti_3C_2(OH)_x$. The Ti and C atoms were in the color of blue and brown, respectively. F atoms in $Ti_3C_2F_x$ were colored in light blue. H atoms in $Ti_3C_2(OH)_x$ were colored in pink. O atoms in $Ti_3C_2O_x$ and $Ti_3C_2(OH)_x$ were colored red.

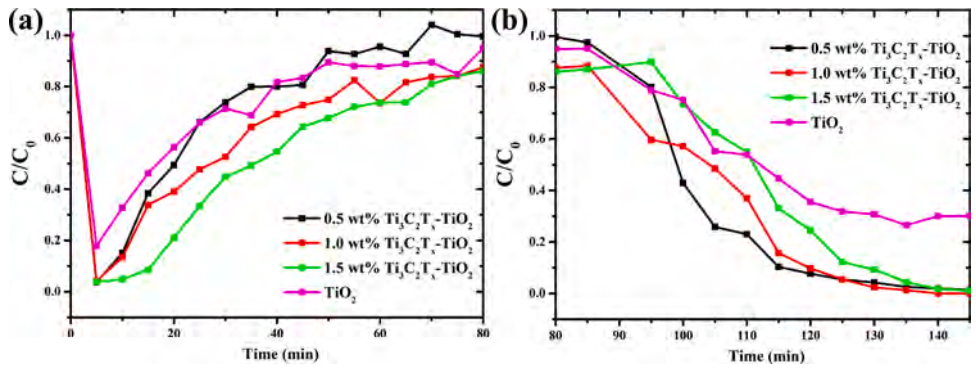

Fig. 5. The adsorption and photocatalytic degradation of acetaldehyde by TiO_2 and the $Ti_3C_2T_x$-TiO_2 composites

$Ti_3C_2T_x$ flakes on the separation of electron-hole pairs in TiO_2 due to its metallic conductivity. As shown by Fig. S20, higher photocurrent density curves are obtained for the $Ti_3C_2T_x$-TiO_2 composites, with the 1.0 wt % $Ti_3C_2T_x$-TiO_2 showing the highest photocurrent density. The photocurrent intensity decreases when further increasing the amount of $Ti_3C_2T_x$, which might be caused by masking effect of $Ti_3C_2T_x$, which, to a certain extent, hinders the utilization of incident light by TiO_2 [54]. The PCO of acetaldehyde by the composite photocatalysts are also characterized (Fig. 5b). Compared with TiO_2, the degradation efficiency increase from ~65% to ~100% when applying $Ti_3C_2T_x$-TiO_2 composites as the photocatalyst, which could be attributed to both the improved adsorption of target molecules and the accelerated separation of electron-hole pairs in TiO_2. These experimental results are in good accordance with our computational results and further confirm the application potential of $Ti_3C_2T_x$ as a co-catalyst in the photocatalytic elimination of indoor air pollutants.

4. Conclusion

In summary, the electronic properties of 2D- Ti_3C_2 sheets and it derivatives with -F, -O and -OH surface terminators are simulated using density functional theory. The adsorption behavior of acetaldehyde molecules on various surfaces have also been explored. Ti_3C_2 with no surface terminators exhibited a strong affiliation to acetaldehyde molecules with a high adsorption energy of 3.64 eV with unsaturated Ti atoms on the surface of Ti_3C_2 working as the active sites for the adsorption of acetaldehyde. Native -F, -O and -OH terminators derived from common synthesis methods tends to dramatically change the adsorption behavior of acetaldehyde. Only physical adsorption of acetaldehyde (with the adsorption energy of ~0.25 eV) happens on the surface of -F and -O terminated $Ti_3C_2T_2$ monolayers, while chemical adsorption could be achieved on the surface of $Ti_3C_2(OH)_2$ (with the adsorption energy of 0.88 eV) due to the H-bond interaction between -OH groups and carbonyl O. Creating T vacancies on the surface of $Ti_3C_2T_2$ by surface modification processes is proven to be an effective way in optimizing its performance in capturing acetaldehyde molecules while maintaining its metallic conductivity and stability in air. After removing a T group from the surface of $Ti_3C_2F_2$, $Ti_3C_2O_2$ and $Ti_3C_2(OH)_2$, the adsorption energy of acetaldehyde increases to 1.750, 1.830 and 1.960 eV, respectively, all higher than the energy needed for the spontaneous capture of acetaldehyde. The specific interaction of carbonyl oxygen with surface Ti or H atoms is found to be the main reason for the chemical adsorption of acetaldehyde by Ti_3C_2 monolayer and its derivatives. In addition to computational results, the application potential of $Ti_3C_2T_x$ flakes as a co-catalyst is also verified by constructing $Ti_3C_2T_x$-TiO_2 composite photocatalysts, which shows improved adsorption and photocatalytic degradation ability toward acetaldehyde. Our work provides a solid foundation for the possibilities of optimizing the performance of $Ti_3C_2T_x$ materials as a co-catalyst for the capture and catalytic elimination of gas molecules by surface modification.

Although providing active absorption sites for acetaldehyde molecules, the T-vacancies still suffer from slow oxidation in air, which limits its long-term application in photocatalysis. The implantation of non-native functional groups such as -P, -S, $-NH_3$, -Cl, et al. might be a promising way in solving this problem. The selection and implantation of a suitable terminators which could both form specific interactions with various target gas molecules and protect the $Ti_3C_2T_x$ flakes from being oxidized is essential for the practical application and leaves further experimental and computational research as a future study.

Appendix A: Supplementary data

Supplementary data (the geometrically optimized structure and DOS of pristine Ti_3C_2 and gas phase acetaldehyde; the DOS for Ti_3C_2 before and after the adsorption of acetaldehyde; the EDD file of Ti_3C_2-acetaldehyde and $Ti_3C_2T_x$ -acetaldehyde complexes; the DOS for $Ti_3C_2T_2$ and $Ti_3C_2T_x$ before and after the adsorption of acetaldehyde; the optimized geometries for the adsorption of acetaldehyde molecules on Ti_3C_2, $Ti_3C_2T_2$ and $Ti_3C_2T_x$, the bond lengths between carbonyl O and surface Ti or H atoms) could be found online at

CRediT authorship contribution statement

Xiao Wang: Conceptualization, Investigation, Validation, Data curation, Formal analysis, Funding acquisition, Writing – original draft. **Asad Mahmood:** Methodology, Formal analysis, Data curation, Writing – original draft. **Gansheng Shi:** Formal analysis, Resources. **Yan Wang:** Data curation. **Guanhong Lu:** Validation, Resources. **Xiaofeng Xie:** Validation, Funding acquisition, Project administration. **Jing Sun:** Methodology, Resources, Funding acquisition, Supervision, Project administration, Writing – review & editing.

Declaration of Competing Interest

The authors declare that they have no known competing financial interests or personal relationships that could have appeared to influence the work reported in this paper.

Acknowledgements

This work was financially supported by the National Key Research and Development Program of China (2016YFA0203000), Shanghai Sailing Program (18YF1426800), the National Natural Science Foundation of China (Grant No. 41907303), the Scientific Research Program of Science and Technology Commission of Shanghai Municipality (Grant No. 19DZ1202600, 20DZ1204100) and the Innovation Project of Shanghai Institute of Ceramics.

Supplementary materials

Supplementary material associated with this article can be found, in the online version, at doi:10.1016/j.surfin.2021.101284.

References

[1] Y. Hu, X. Xie, X. Wang, Y. Wang, Y. Zeng, D.Y.H. Pui, J. Sun, Visible-light upconversion carbon quantum dots decorated TiO_2 for the photodegradation of flowing gaseous acetaldehyde, Appl. Surf. Sci. 440 (2018) 266–274, https://doi.org/10.1016/j.apsusc.2018.01.104.

[2] W. Lin, X. Xie, X. Wang, Y. Wang, D. Segets, J. Sun, Efficient adsorption and sustainable degradation of gaseous acetaldehyde and O-xylene using rGO-TiO_2 photocatalyst, Chem. Eng. J. 349 (2018) 708–718, https://doi.org/10.1016/j.cej.2018.05.107.

[3] A.H. Mamaghani, F. Haghighat, C.-S. Lee, Photocatalytic oxidation technology for indoor environment air purification: the state-of-the-art, Appl. Catal. B 203 (2017) 247–269, https://doi.org/10.1016/j.apcatb.2016.10.037.

[4] J. Mo, Y. Zhang, Q. Xu, J.J. Lamson, R. Zhao, Photocatalytic purification of volatile organic compounds in indoor air: a literature review, Atmos. Environ. 43 (14) (2009) 2229–2246, https://doi.org/10.1016/j.atmosenv.2009.01.034.

[5] Z. Shayegan, C.-S. Lee, F. Haghighat, TiO_2 photocatalyst for removal of volatile organic compounds in gas phase – a review, Chem. Eng. J. 334 (2018) 2408–2439, https://doi.org/10.1016/j.cej.2017.09.153.

[6] Y. Huang, P. Wang, Z. Wang, Y. Rao, J.-j. Cao, S. Pu, W. Ho, S.C. Lee, Protonated g-C_3N_4/Ti^{3+}_3 sel-Fdoped TiO_2 nanocomposite films: Room-temperature preparation, hydrophilicity, and application for photocatalytic NO removal, Appl. Catal. B 240 (2019) 122–131, https://doi.org/10.1016/j.apcatb.2018.08.078.

[7] Y. Yan, M. Han, A. Konkin, T. Koppe, D. Wang, T. Andreu, G. Chen, U. Vetter, J. R. Morante, P. Schaaf, Slightly hydrogenated TiO_2 with enhanced photocatalytic performance, J. Mater. Chem. A 2 (32) (2014) 12708–12716, https://doi.org/10.1039/c4ta02192d.

[8] L. Han, B. Su, G. Liu, Z. Ma, X. An, Synthesis of oxygen vacancy-rich black TiO_2 nanoparticles and the visible light photocatalytic performance, Mol. Catal. 456 (2018) 96–101, https://doi.org/10.1016/j.mcat.2018.07.006.

[9] Y. Wang, J. Yu, W. Peng, J. Tian, C. Yang, Novel multilayer TiO_2 heterojunction decorated by low g-C3N4 content and its enhanced photocatalytic activity under UV, visible and solar light irradiation, Sci. Rep. 9 (1) (2019) 5932, https://doi.org/10.1038/s41598-019-42438-w.

[10] Y. Boyjoo, H. Sun, J. Liu, V.K. Pareek, S. Wang, A review on photocatalysis for air treatment: From catalyst development to reactor design, Chem. Eng. J. 310 (2017) 537–559, https://doi.org/10.1016/j.cej.2016.06.090.

[11] X. Dai, Y. Wang, X. Wang, S. Tong, X. Xie, Polarity on adsorption and photocatalytic performances of N-GR/TiO_2 towards gaseous acetaldehyde and ethylene, Appl. Surf. Sci. 485 (2019) 255–265, https://doi.org/10.1016/j.apsusc.2019.04.221.

[12] C.H. Ao, S.C. Lee, Combination effect of activated carbon with TiO_2 for the photodegradation of binary pollutants at typical indoor air level, J. Photochem. Photobiol. A 161 (2) (2004) 131–140, https://doi.org/10.1016/S1010-6030(03)00276-4.

[13] L.-M. Liu, P. Crawford, P. Hu, The interaction between adsorbed OH and O_2 on TiO_2 surfaces, Prog. Surf. Sci. 84 (5) (2009) 155–176, https://doi.org/10.1016/j.progsurf.2009.01.002.

[14] K. Hashimoto, H. Irie, A. Fujishima, TiO_2 Photocatalysis: a historical overview and future prospects, Japan. J. Appl. Phys. 44 (12) (2005) 8269–8285, https://doi.org/10.1143/jjap.44.8269.

[15] M. Zhao, Y. Huang, Y. Peng, Z. Huang, Q. Ma, H. Zhang, Two-dimensional metal-organic framework nanosheets: synthesis and applications, Chem. Soc. Rev. 47 (16) (2018) 6267–6295, https://doi.org/10.1039/c8cs00268a.

[16] Y. Zhang, L. Wang, N. Zhang, Z. Zhou, Adsorptive environmental applications of MXene nanomaterials: a review, RSC Adv. 8 (36) (2018) 19895–19905, https://doi.org/10.1039/c8ra03077d.

[17] M. Naguib, V.N. Mochalin, M.W. Barsoum, Y. Gogotsi, 25th anniversary article: MXenes: a new family of two-dimensional materials, Adv. Mater. 26 (7) (2014) 992–1005, https://doi.org/10.1002/adma.201304138.

[18] H. Lin, Y. Wang, S. Gao, Y. Chen, J. Shi, Theranostic 2D tantalum carbide (MXene), Adv. Mater. 30 (4) (2018), https://doi.org/10.1002/adma.201703284.

[19] Hong Ng, V. M., H. Huang, K. Zhou, P.S. Lee, W. Que, J.Z. Xu, L.B Kong, Recent progress in layered transition metal carbides and/or nitrides (MXenes) and their composites: synthesis and applications, J. Mater. Chem. A 5 (7) (2017) 3039–3068, https://doi.org/10.1039/c6ta06772g.

[20] M. Khazaei, A. Mishra, N.S. Venkataramanan, A.K. Singh, S. Yunoki, Recent advances in MXenes: from fundamentals to applications, Curr. Opin. Solid State Mater. Sci. 23 (3) (2019) 164–178, https://doi.org/10.1016/j.cossms.2019.01.002.

[21] A. Feng, Y. Yu, Y. Wang, F. Jiang, Y. Yu, L. Mi, L. Song, Two-dimensional MXene Ti_3C_2 produced by exfoliation of Ti_3AlC_2, Mater. Des. 114 (2017) 161–166, https://doi.org/10.1016/j.matdes.2016.10.053.

[22] M. Naguib, M. Kurtoglu, V. Presser, J. Lu, J. Niu, M. Heon, L. Hultman, Y. Gogotsi, M.W. Barsoum, Two-dimensional nanocrystals produced by exfoliation of Ti_3 AlC_2, Adv. Mater. 23 (37) (2011) 4248–4253, https://doi.org/10.1002/adma.201102306.

[23] L.M. Azofra, N. Li, D.R. MacFarlane, C. Sun, Promising prospects for 2D d2–d4 $M3C_2$ transition metal carbides (MXenes) in N2 capture and conversion into ammonia, Energy Environ. Sci. 9 (8) (2016) 2545–2549, https://doi.org/10.1039/c6ee01800a.

[24] S.J. Kim, H.J. Koh, C.E. Ren, O. Kwon, K. Maleski, S.Y. Cho, B. Anasori, C.K. Kim, Y. K. Choi, J. Kim, Y. Gogotsi, H.T. Jung, Metallic Ti_3C_2Tx MXene gas sensors with ultrahigh signal-to-noise ratio, ACS nano 12 (2) (2018) 986–993, https://doi.org/10.1021/acsnano.7b07460.

[25] F. Liu, A. Zhou, J. Chen, J. Jin, W. Zhou, L. Wang, Q. Hu, Preparation of Ti_3C_2 and Ti_2C MXenes by fluoride salts etching and methane adsorptive properties, Appl. Surf. Sci. 416 (2017) 781–789, https://doi.org/10.1016/j.apsusc.2017.04.239.

[26] N. Li, X. Chen, W.J. Ong, D.R. MacFarlane, X. Zhao, A.K. Cheetham, C. Sun, Understanding of electrochemical mechanisms for CO_2 capture and conversion into hydrocarbon fuels in transition-metal carbides (MXenes), ACS nano 11 (11) (2017) 10825–10833, https://doi.org/10.1021/acsnano.7b03738.

[27] L. Ding, Y. Wei, L. Li, T. Zhang, H. Wang, J. Xue, L.-X. Ding, S. Wang, J. Caro, Y. Gogotsi, MXene molecular sieving membranes for highly efficient gas separation, Nat. Commun. 9 (2018), https://doi.org/10.1038/s41467-017-02529-6.

[28] J. Low, L. Zhang, T. Tong, B. Shen, J. Yu, TiO_2/MXene Ti_3C_2 composite with excellent photocatalytic CO_2 reduction activity, J. Catal. 361 (2018) 255–266, https://doi.org/10.1016/j.jcat.2018.03.009.

[29] A. Shahzad, K. Rasool, M. Nawaz, W. Miran, J. Jang, M. Moztahida, K. A. Mahmoud, D.S. Lee, Heterostructural TiO_2/$Ti_3C_2T_x$ (MXene) for photocatalytic degradation of antiepileptic drug carbamazepine, Chem. Eng. J. 349 (2018) 748–755, https://doi.org/10.1016/j.cej.2018.05.148.

[30] C. Peng, X. Yang, Y. Li, H. Yu, H. Wang, F. Peng, Hybrids of two-dimensional Ti_3C_2 and TiO_2 exposing 001 facets toward enhanced photocatalytic activity, ACS Appl. Mater. Interfaces 8 (9) (2016) 6051–6060, https://doi.org/10.1021/acsami.5b11973.

[31] M. Okubo, A. Sugahara, S. Kajiyama, A. Yamada, MXene as a charge storage host, Acc. Chem. Res. 51 (3) (2018) 591–599, https://doi.org/10.1021/acs.accounts.7b00481.

[32] Z. Ai, Y. Shao, B. Chang, L. Zhang, J. Shen, Y. Wu, B. Huang, X. Hao, Rational modulation of p-n homojunction in P-doped g-C_3N_4 decorated with Ti_3C_2 for photocatalytic overall water splitting, Appl. Catal. B 259 (2019), 118077, https://doi.org/10.1016/j.apcatb.2019.118077.

[33] Z. Guo, J. Zhou, L. Zhu, Z. Sun, MXene: a promising photocatalyst for water splitting, J. Mater. Chem. A 4 (29) (2016) 11446–11452, https://doi.org/10.1039/c6ta04414j.

[34] Y. Li, X. Deng, J. Tian, Z. Liang, H. Cui, Ti_3C_2 MXene-derived Ti_3C_2/TiO_2 nanoflowers for noble-metal-free photocatalytic overall water splitting, Appl. Mater. Today 13 (2018) 217–227, https://doi.org/10.1016/j.apmt.2018.09.004.

[35] Y. Gao, L. Wang, A. Zhou, Z. Li, J. Chen, H. Bala, Q. Hu, X. Cao, Hydrothermal synthesis of TiO_2/Ti_3C_2 nanocomposites with enhanced photocatalytic activity, Mater. Lett. 150 (2015) 62–64, https://doi.org/10.1016/j.matlet.2015.02.135.

[36] X.J. Zha, X. Zhao, J.H. Pu, L.S. Tang, K. Ke, R.Y. Bao, L. Bai, Z.Y. Liu, M.B. Yang, W. Yang, Flexible anti-biofouling MXene/cellulose fibrous membrane for sustainable solar-driven water purification, ACS Appl. Mater. Interfaces (2019), https://doi.org/10.1021/acsami.9b10606.

[37] Y. Gao, H. Chen, A. Zhou, Z. Li, F. Liu, Q. Hu, L. Wang, Novel hierarchical TiO_2/C nanocomposite with enhanced photocatalytic performance, Nano 10 (05) (2015), 1550064, https://doi.org/10.1142/s1793292015500642.

[38] Z.H. Fu, Q.F. Zhang, D. Legut, C. Si, T.C. Germann, T. Lookman, S.Y. Du, J. S. Francisco, R.F. Zhang, Stabilization and strengthening effects of functional groups in two-dimensional titanium carbide, Phys. Rev. B 94 (10) (2016), https://doi.org/10.1103/PhysRevB.94.104103.

[39] M. Khazaei, A. Ranjbar, M. Arai, T. Sasaki, S. Yunoki, Electronic properties and applications of MXenes: a theoretical review, J. Mater. Chem. C 5 (10) (2017) 2488–2503, https://doi.org/10.1039/c7tc00140a.

[40] T. Schultz, N.C. Frey, K. Hantanasirisakul, S. Park, S.J. May, V.B. Shenoy, Y. Gogotsi, N. Koch, Surface termination dependent work function and electronic properties of $Ti_3C_2T_x$ MXene, Chem. Mater. (2019), https://doi.org/10.1021/acs.chemmater.9b00414.

[41] M. Naguib, M. Kurtoglu, V. Presser, J. Lu, J. Niu, M. Heon, L. Hultman, Y. Gogotsi, M.W. Barsoum, Two-dimensional nanocrystals produced by exfoliation of Ti_3AlC_2, Adv. Mater. 23 (37) (2011) 4248–4253, https://doi.org/10.1002/adma.201102306.

[42] S. Tu, Q. Jiang, J. Zhang, X. He, M.N. Hedhili, X. Zhang, H.N. Alshareef, Enhancement of dielectric permittivity of Ti_3C_2Tx MXene/polymer composites by controlling flake size and surface termination, ACS Appl. Mater. Interfaces (2019), https://doi.org/10.1021/acsami.9b09137.

[43] V. Natu, R. Pai, M. Sokol, M. Carey, V. Kalra, M.W. Barsoum, 2D Ti_3C_2Tz MXene synthesized by water-free etching of Ti_3AlC_2 in polar organic solvents, Chemistry 6 (3) (2020) 616–630, https://doi.org/10.1016/j.chempr.2020.01.019.

[44] P. Liu, W. Ding, J. Liu, L. Shen, F. Jiang, P. Liu, Z. Zhu, G. Zhang, C. Liu, J. Xu, Surface termination modification on high-conductivity MXene film for energy conversion, J. Alloys Compd. 829 (2020), https://doi.org/10.1016/j.jallcom.2020.154634.

[45] F.M. Roemer, U. Wiedwald, T. Strusch, J. Halim, E. Mayerberger, M.W. Barsoum, M. Farle, Controlling the conductivity of Ti_3C_2 MXenes by inductively coupled oxygen and hydrogen plasma treatment and humidity, RSC Adv. 7 (22) (2017) 13097–13103, https://doi.org/10.1039/c6ra27505b.

[46] H. Tang, Y. Yang, R. Wang, J. Sun, Improving the properties of 2D titanium carbide films by thermal treatment, J. Mater. Chem. C 8 (18) (2020) 6214–6220, https://doi.org/10.1039/C9TC07018D.

[47] I. Persson, L.-A. Naslund, J. Halim, M.W. Barsoum, V. Darakchieva, J. Palisaitis, J. Rosen, P.O.A. Persson, On the organization and thermal behavior of functional groups on Ti_3C_2 MXene surfaces in vacuum, 2d Materials 5 (1) (2018), https://doi.org/10.1088/2053-1583/aa89cd.

[48] G. Kresse, J. Furthmüller, Efficient iterative schemes for ab initio total-energy calculations using a plane-wave basis set, Phys. Rev. B 54 (16) (1996) 11169–11186, https://doi.org/10.1103/PhysRevB.54.11169.

[49] S. Grimme, J. Antony, S. Ehrlich, H. Krieg, A consistent and accurate ab initio parametrization of density functional dispersion correction (DFT-D) for the 94 elements H-Pu, J. Chem. Phys. 132 (15) (2010), 154104, https://doi.org/10.1063/1.3382344.

[50] J.P. Perdew, K. Burke, M. Ernzerhof, Generalized gradient approximation made simple, Phys. Rev. Lett. 77 (18) (1996) 3865–3868, https://doi.org/10.1103/PhysRevLett.77.3865.

[51] H.J. Monkhorst, J.D. Pack, Special points for Brillouin-zone integrations, Phys. Rev. B 13 (12) (1976) 5188–5192, https://doi.org/10.1103/PhysRevB.13.5188.

[52] H. Guo, W. Zhang, N. Lu, Z. Zhuo, X.C. Zeng, X. Wu, J. Yang, CO_2 Capture on h-BN sheet with high selectivity controlled by external electric field, J. Phys. Chem. C 119 (12) (2015) 6912–6917, https://doi.org/10.1021/acs.jpcc.5b00681.

[53] Q. Tang, Z. Zhou, P. Shen, Are MXenes promising anode materials for Li ion batteries? Computational studies on electronic properties and Li storage capability of Ti_3C_2 and $Ti3C_2 \times 2$ (X = F, OH) monolayer, J. Am. Chem. Soc. 134 (40) (2012) 16909–16916, https://doi.org/10.1021/ja308463r.

[54] T. Su, Z.D. Hood, M. Naguib, L. Bai, S. Luo, C.M. Rouleau, I.N. Ivanov, H. Ji, Z. Qin, Z. Wu, Monolayer Ti_3C_2Tx as an effective co-catalyst for enhanced photocatalytic hydrogen production over TiO_2, ACS Appl. Energy Mater. 2 (7) (2019) 4640–4651.